energy&fuels Article
Cite This: Energy Fuels 2019, 33, 7604−7613 pubs.acs.org/EF

Experimental Study on Spontaneous Imbibition of CO_2-Rich Brine in Tight Oil Reservoirs

Yongqiang Tang,[†] Rui Wang,[†] Zihao Li,[‡] Maolei Cui,[†] Zengmin Lun,[†] and Yu Lu*[,§]

[†]Petroleum Exploration and Production Research Institute, Sinopec, Beijing 100083, China
[‡]Department of Mining and Minerals Engineering, Virginia Tech, Blacksburg, Virginia 24061, United States
[§]School of Business, Beijing Technology and Business University, Beijing 100048, China

ABSTRACT: This paper focuses on the CO_2-EOR in fractured tight oil reservoirs after water-flooding treatment. In previous works, few studies were presented about the spontaneous imbibition experiments of CO_2-rich brine at formation pressure. We investigated the influence of CO_2 injection on spontaneous imbibition, which is an essential mechanism to improve oil recovery in tight reservoir. In this paper, a laboratory equipment was set up to conduct spontaneous imbibition experiments at formation temperature of 65 °C and pressures of 10−22 MPa on different low-permeability core samples from Nugget, Kentucky, Colton, and Crab-Orchard in the United States. Moreover, we proposed a saturation-based dimensionless time model to scale the spontaneous imbibition and a modified Ma model to fit the oil recovery curves of spontaneous imbibition of CO_2-rich brine with double peaks of imbibition rate. The results of quantitative imbibition experiments confirm that both the oil production per unit area and the oil recovery have a positive proportional relationship with permeability. A primary reason is that both the capillary pressure and the viscous resistance increase with decreasing of capillary size, but the viscous resistance is more sensitive. The result also quantitatively demonstrates that both the oil production and the oil recovery increase with confining pressure, especially when the pressure exceeds minimum miscibility pressure. However, the pendent drop test illustrates that CO_2 decreases the oil−water interfacial tension with the elevating of pressure. CO_2 can improve the recovery of tight oil by spontaneous imbibition in two main mechanisms: decreasing oil viscosity to improve flowing ability and oil swelling to enhance the cocurrent imbibition. This work provides theory basis and feasible measure for CO_2-EOR in the fractured and water-flooded tight reservoir.

1. INTRODUCTION

Tight oil is a new unconventional resource and has emerged as a significant source of energy supply in the world.[1] With the development of horizontal well and hydraulic fracturing technologies, the production of tight oil has increased significantly since 2010.[2] In the U.S., tight oil is mainly explored in seven basins (see Figure 1a). The U.S. Energy Information Administration reported that as of 2017 the production of tight oil had increased to more than 4 million barrels per day (b/d), making up 49.71% of total oil production in U.S., and it is expected to reach 11.0 million b/d by 2035, or 66% of total U.S. production.[3,4] In China, tight oil has also been explored in many basins (see Figure 1b). According to the data from Strategic Research Center of Oil and Gas Resources of Ministry of Natural Resources of China, tight oil in China has a recoverable oil reservoir of 2−2.5 billion ton, which occupied 2/5 of the total recoverable oil reservoir of China.[5,6] Especially, the tight resources in Yanchang Formation of the Ordos Basin have a proven geological reservoir of about 2 billion ton[5] and have a production increasing to about 647.5 t/d by 2016.[7] As the production increases rapidly, tight oil has become a new hot spot of oil exploration and development after shale oil.[2]

The oilfield application found that oil production of water flooding with horizontal well fracturing decreased rapidly due to the low injectivity and poor sweep efficiency,[13] especially for some oil-wet tight formations.[4] Compared with conventional reservoirs, tight oil reservoirs are typically characterized by low porosity and low permeability.[9] Thus, the multistage hydraulic fracturing technologies are widely applied in the development of tight oil in recent years. Hydraulic fracturing often builds a dual-pore system, in which the fracture system would provide a conductive system.[1] However, most hydrocarbons are stored in the tight matrix.[10,11] Spontaneous imbibition is one of the main mechanisms to displace oil in the tight porous medium and plays a significant role in unlocking tight oil potentials as a tremendous amount of oil remains in the matrix after primary production.[12] The ability of spontaneous imbibition is critical for the successful development of tight oil reservoirs.[11]

It is known that spontaneous imbibition occurs in two types: countercurrent and cocurrent imbibition.[13,14] Capillary pressure is the most dominated power to drive spontaneous imbibition in the fractured tight reservoir.[15] When the tight matrix is covered by brine, the production of oil will be contributed by both countercurrent and cocurrent imbibition. The countercurrent imbibition is defined as being when the displacing wetting fluid flows in the opposite direction to the produced nonwetting fluid, which is caused by the disproportion of capillary pressure, since fracture networks are generally heterogeneous. The cocurrent imbibition is the flow of wetting and nonwetting phase in the same direction which is driven by capillary pressure and other forces (e.g.,

Received: May 21, 2019
Revised: July 18, 2019
Published: July 23, 2019

DOI: 10.1021/acs.energyfuels.9b01621
Energy Fuels 2019, 33, 7604−7613

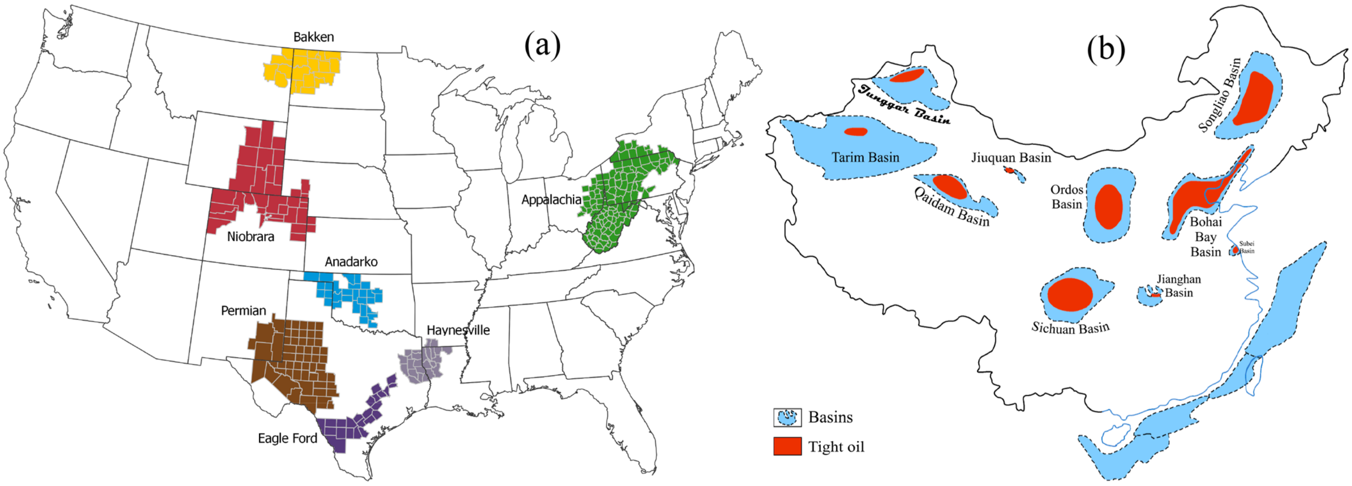

Figure 1. Distribution in main basins of tight oil in U.S. and China.[3,8]

gravity). The imbibition rate of countercurrent imbibition is usually higher than cocurrent imbibition while the cocurrent imbibition is generally more continuous.[15]

Carbon dioxide (CO_2) is considered as an injection strategy for enhanced oil recovery (EOR) in tight oil reservoirs. The growing concern about CO_2 emission promotes the development of CO_2-EOR technologies with both miscible and immiscible. Many experimental and simulation studies[16−27] have shown that $scCO_2$ injection is one of the most effective and feasible methods to improve oil recovery in water-flooded formation. CO_2-EOR mechanisms in the conventional reservoir for both CO_2 flooding and CO_2 huff-n-puff are well understood,[9] including soluble in brine, oil viscosity reduction, oil swelling, light-hydrocarbons extraction, oil−gas interfacial tension (IFT) reduction, exerting an acid effect on rock, etc.[4,17] However, the nonwetted $scCO_2$ will flow along with fractures and is hard to flow into the tight matrix which is filled with fluids. It is well accepted that the CO_2-EOR process in tight oil formation has several conceptual steps:[4,9] (1) The injected $scCO_2$ flows into the fractures, and the rock matrix is exposed to $scCO_2$ at fracture surfaces. (2) The scCO2 diffuses into the crude oil in the porous rocks[18] and then the swelling of crude oil extrudes some oil out of the pores.[19] (3) The oil migrates to the bulk $scCO_2$ in the fractures with swelling and reduced viscosity. (4) As pressure is dropped, the dissolved CO_2 slowly drives oil from the pores into the bulk $scCO_2$ in the fractures.

The large amounts of brine in the hydraulic fracturing can be trapped in the pore space of the rock which leads to the surface pore of the tight matrix filled with brine.[1] Moreover, because the fractured tight reservoirs have often been developed with long-term water-flooding treatment, the covered brine will restrain the vaporization of oil components into $scCO_2$. Such water-covered boundary conditions have received much attention with regard to the mechanisms of oil production and scaling of imbibition.[13] Therefore, it is crucial to study the CO_2-EOR mechanisms in water-flooded tight reservoirs.

However, few studies of this topic have been presented before. Some researchers believed that the influence of CO_2 on spontaneous brine imbibition is a key issue.[21,22] Wang et al. (2010)[21] found that the dissolved $scCO_2$ was beneficial to switch the tight sandstone from oil-wet toward water-wet to improve the recovery of spontaneous brine imbibition. Yang et al. (2015)[22] found $scCO_2$ can improve fluid injectivity in tight reservoir with the mechanisms of carbonate material solubility and retarding clay swelling.

In our previous work,[27] we investigated the effect of water barrier on CO_2 flooding on the basis of microscopic experiments on ideal porous models. We found that the $scCO_2$ can diffuse into the oil through brine barrier and confirmed the microscopic mechanism of CO_2-EOR on trapped oil droplets with several steps, including dissolution, swelling, extraction, and multiple contact miscibility. Therefore, we believe that the dissolution of CO_2 can enhance spontaneous imbibition. In this paper, spontaneous imbibition experiments are conducted on tight core samples with different permeability under different pressures of 10−22 MPa for further clarifying the mechanisms of CO_2-EOR into the water-flooded tight reservoirs and the influence of permeability and pressure.

2. EXPERIMENTAL SECTION

2.1. Materials. The spontaneous imbibition experiments are conducted under the formation conditions of tight oil reservoir, Yanchang Formation, southern of Ordos Basin. The average formation temperature is 65 °C. The formation pressures are in the range of 9.68−22.83 MPa (average, 18.2 MPa). The live oil has a bubble-point pressure of 6.35 MPa. Its viscosity is 1.05−3.41 mPa·s, and its density is 0.783−0.861 g/cm^3 under formation conditions.[28−36]

The natural gas is rich gas from Yanchang Formation provided by the Honghe Oilfield, Sinopec. Its component determined with gas chromatography (Water, U.S.) is depicted in Figure 2.

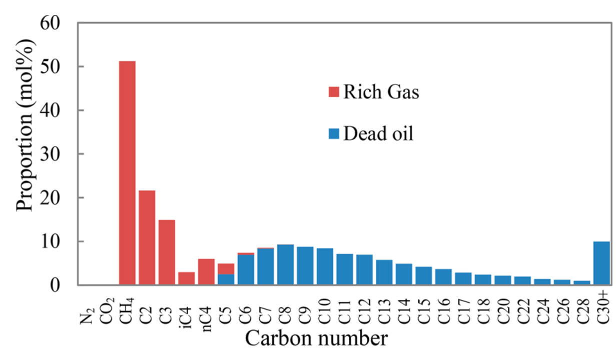

Figure 2. Component of natural gas and dead oil fractions.[32]

DOI: 10.1021/acs.energyfuels.9b01621
Energy Fuels 2019, 33, 7604−7613

The oil sample is stock tank oil from Yanchang Formation offered by Honghe Oilfield, Sinopec. The minimum miscibility pressure of dead oil to CO_2 is 19.32 MPa tested with slim tube system (VINCI, France) is 20.97 MPa tested with IFT 1000 (S.T., Core Lab, U.S.) under 65 °C. The viscosity measured with a MCR 302 rheometer (Anton Paar, US) is 2.90 mPa·s under 65 °C and 0.1 MPa, and the viscosity is 7.81 mPa·s under 20 °C and 0.1 MPa. The crude oil has a density of 0.757 g/cm^3 (DMA 4500, Anton Paar, U.S.) under 65 °C.[28−32] The distribution of oil fractions is depicted in Figure 2.

The brine was provided by the Honghe Oilfield, Sinopec. The salinity of resident brine is 55.309 mg/L. The ionic composition is listed in Table 1.

Table 1. Ionic Composition of the Brine Sample

Na^+ and K^+	Ca^{2+}	Mg^{2+}	Cl^-	HCO_3^-	total	type
18766	1711	722	33879	231	55309	$CaCl_2$

The CO_2 was purchased from Beijing Huayuan Gas Chemical Industry Co. Ltd. (China) and has a purity higher than 99.99 mol %.

Four typical tight reservoirs are used to investigate the influence of porous structure on spontaneous imbibition. The standard core samples taken from Nugget, Kentucky, Colton, and Crab Orchard are purchased through Beijing Huashenghaitian Technology Co., Ltd. (China). The parameters of the cores used in this paper are listed in Table 2.

2.2. Apparatus. A laboratory equipment was designed to conduct spontaneous imbibition experiments of CO_2-rich brine into the tight reservoirs at formation temperature and pressure (Figure 3).

The apparatus has a pressure cell made of Hastelloy alloy for bearing 150 MPa pressure. The cell has a cavity with inside diameters of 5 cm and length of 25 cm. The container wall is 3 cm thickness. A bottom cover, sealed with O-ring, is used for convenient loading core samples. There is a bottom valve at the bottom of the cavity and a sampling valve at the upper.

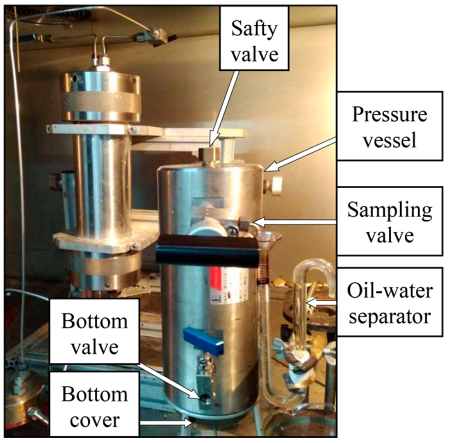

Figure 3. Photograph of spontaneous imbibition apparatus.

2.3. Experimental Procedures. The spontaneous imbibition experiments of CO_2-rich brine are conducted on the tight cores. By the experiments, we can obtain the variation rule of oil recovery and oil production rate with time to explore the influence of CO_2. The experimental procedures are described as follows:

(a) After the size and weight are measured, the dry clean core samples are positioned in a pressure tank and vacuumized to the pressure below 10^{-7}Pa with a molecular vacuum pump (Pfeiffer HiCube, Germany) for more than 72 h.

Table 2. Detailed Parameters of the Core Samples

core samples	no.	length (mm)	diameter (mm)	surface area (mm^2)	Φ_{He} (%)	K_{He} (mD)	K/Φ (μm)	L_c (mm)
Nugget sandstone	N-1	101.86	38.24	14533.9	9.6575	0.9991	0.1017	17.075
	N-2	101.84	38.23	14527.1	9.6564	0.9992	0.1017	17.067
	N-3	101.80	38.28	14544.3	9.6845	0.9991	0.1016	17.107
Kentucky sandstone	K-1	100.13	38.23	14321.7	13.9187	0.1051	0.0275	17.028
	K-2	100.15	38.25	14332.8	14.0384	0.1056	0.0274	17.045
	K-3	99.90	38.20	14281.1	14.0825	0.1048	0.0273	16.998
	K-4	99.87	38.25	14299.1	13.9623	0.1055	0.0275	17.039
	K-5	99.86	38.24	14293.6	13.9365	0.1055	0.0275	17.03
	K-6	100.35	38.22	14343.8	14.0336	0.1051	0.0274	17.025
	K-7	100.49	38.23	14364.9	13.7768	0.1052	0.0276	17.036
	K-8	100.00	38.19	14288.7	13.6828	0.1046	0.0276	16.992
	K-9	100.66	38.26	14398.4	13.6585	0.1058	0.0278	17.065
	K-A	99.91	38.23	14295.3	14.2016	0.1052	0.0272	17.023
	K-B	100.37	38.23	14350.5	13.8262	0.1052	0.0276	17.034
	K-C	100.23	38.21	14325.0	14.3612	0.1049	0.0270	17.014
	K-D	99.80	38.24	14286.4	14.5288	0.1053	0.0269	17.029
	K-E	100.04	38.23	14310.9	14.4773	0.1053	0.0270	17.026
	K-F	100.57	38.22	14370.2	14.5031	0.1051	0.0269	17.03
	K-G	100.33	38.22	14341.4	14.1643	0.1051	0.0272	17.024
	K-H	100.53	38.22	14365.4	14.2863	0.1051	0.0271	17.029
	K-I	100.08	38.19	14298.3	14.2579	0.1045	0.0271	16.994
	K-J	100.52	38.22	14364.2	14.3184	0.1050	0.0271	17.029
	K-K	100.31	38.27	14360.7	14.0857	0.1060	0.0274	17.065
Colton sandstone	C-1	101.80	38.26	14535.5	12.4928	0.0530	0.0206	17.091
	C-2	101.80	38.23	14522.3	12.5815	0.0541	0.0207	17.066
	C-3	101.52	38.28	14510.6	12.1036	0.0512	0.0206	17.101
Crab Orchard sandstone	Co-1	100.00	38.21	14297.4	5.6239	0.0119	0.0146	17.008
	Co-2	100.40	38.22	14349.8	5.5957	0.0118	0.0145	17.026
	Co-3	100.30	38.21	14333.4	5.7048	0.0119	0.0145	17.015

DOI: 10.1021/acs.energyfuels.9b01621
Energy Fuels 2019, 33, 7604−7613

(b) We inject dead oil into the tank to prepare the oil-saturated samples. After heating to 65 °C in a calorstat and pressurizing the tank to 20 MPa with dead oil, the original wettability of the core samples can be rebuilt through optimum aging for more than 30 days.
(c) After the oil saturation is measured by weight method, we place two oil-saturated core plugs in the pressure cell (Figure 3) with all surfaces in contact with gas. We blow natural gas into the cell and exhaust the air; raise temperature to 65 °C with the calorstat and elevate pressure to experimental pressure by injecting natural gas with a constant pressure pump (VINCI, France).
(d) After the thermodynamic equilibrium is reached, we inject CO_2 solution prepared at experimental pressure and temperature (65 °C) from the bottom valve and exhaust the natural gas from sampling valve until water breakthrough, during which the pressure remains constant. Due to the hole of the sampling valve being 2 mm from the top of the cavity, a gas cap will form, and the core plugs can completely submerge in the CO_2 solution with all surfaces in contact with CO_2-rich brine.
(e) Maintaining the pressure constant, we inject $scCO_2$ into cell from the bottom valve to blow other gases out of the gas cap from the sampling valve for several minutes. In steps (d) and (e), the oil production is eliminated from initial reserve of core plugs and also not included in total production.
(f) The spontaneous imbibition is conducted with pressure remaining constant by supplying $scCO_2$ from the bottom valve. At regular intervals, the oil is taken from the sampling valve with pressure constant to determine the oil production. During the sampling process, the oil below the position of sampling valve is flooded by CO_2 solution, and the oil above the valve is flooded with $scCO_2$.
(g) At early stage, we perform close sampling, and sampling period is gradually extended with the slowdown of the oil production rate. The oil recovery and oil production rate of spontaneous imbibition are calculated to obtain their variation rule with time.

3. MATHEMATICAL MODEL

3.1. Saturation-Based Dimensionless Time Model. The Young–Laplace equation is the most common model to describe capillary pressure.

$$P_c = \frac{2\sigma \cos\theta}{r_c} \tag{1}$$

where σ is interfacial tension, $N\cdot m^{-1}$, θ is contact angle, and r_c is capillary radius, m.

Aronofsky model is an exponential model to fit the oil recovery of spontaneous imbibition in fractured reservoirs.[38]

$$E_R = E_R^{max}(1 - e^{-\lambda t}) \tag{2}$$

where E_R is oil recovery, E_R^{max} is ultimate oil recovery, λ is power index, and t is imbibition time, s.

The oil recovery (E_R) model is modified by using ultimate oil recovery (E_R^{max}) and dimensionless time (t_D). Some common oil recovery models of spontaneous imbibition are listed in Table 3.

Dimensionless time is widely used for scaling spontaneous imbibition on fractured reservoirs.[35] Some common equations of dimensionless time are listed in Table 4.

For any sample shape and boundary conditions, the characteristic capillary length is

$$L_c = \sqrt{V_b / \sum_{i=1}^{n} \frac{A_i}{l_{A_i}}} \tag{3}$$

Table 3. Common Oil Recovery Models of Spontaneous Imbibition[a]

research	formula	value of parameters
Ma et al. (1997)[39]	$E_R = E_R^{max}(1 - e^{-\lambda t_D})$	$\lambda = 0.05$,[39] 0.5[40]
Viksund et al. (2004)[41]	$E_R = E_R^{max}[1 - (1 + at_D)^{-\lambda}]$	$a = 0.04$, $\lambda = 1.5$[1,41]
Babadagli et al. (2009)[42]	$E_R = E_R^{max}(1 - e^{-\omega t_D^n})$	
Standnes (2010)[43]	$E_R = E_R^{max}(1 - We^{-1-\lambda t_D})$	$\lambda = 0.0135$[43]

[a] t_D is dimensionless time; λ, a, ω, n, and W are model parameters.

where V_b is the bulk volume of core sample, m^3, A_i the area perpendicular to the ith imbibition direction, m^2, and l_{Ai} the distance from A_i to the no-flow boundary, m.

Based on the Young–Laplace equation (eq 1) and the Hagen–Poiseuille equation, the spontaneous imbibition in an ideal simple capillary tube can be described as

$$\frac{2\sigma\cos\theta}{r_c} = \frac{8Q\mu L_c}{\pi r_c^4} + \Delta\rho g x \sin\phi \tag{4}$$

where Q is flow rate, $m^3\cdot s^{-1}$, $\Delta\rho$ is density difference, $kg\cdot m^{-3}$, g is gravity, φ is the dip angle of capillary tube, and μ is geometric mean of water and oil viscosities, Pa·s.

In tight reservoir, the gravity is weak enough to ignore comparing with capillary force. Ignoring gravity, the Washburn's equation describes flow in a bundle of parallel capillary tubes.

$$L_c = \sqrt{\frac{cr_c\sigma\cos\theta}{2\mu}t} \tag{5}$$

The average viscosity is a key parameter to measure dimensionless time. The average viscosity of fluid in sweep region is concerned with the saturation excluding the irreducible and residual saturation.

$$\mu = \mu_w S'_w + \mu_{nw} S'_{nw},\ S'_w = \frac{S_w - S_{iw}}{1 - S_{rnw} - S_{iw}}$$
$$S'_{nw} = \frac{S_{nw} - S_{rnw}}{1 - S_{rnw} - S_{iw}} \tag{6}$$

where S'_w is normalized saturation to wetting phase, S'_{nw} is normalized saturation to nonwetting phase, S_w is wetting phase saturation, S_{iw} is irreducible wetting phase saturation, S_{rnw} is residual nonwetting phase saturation, and S_{nw} is nonwetting phase saturation.

Therefore, we proposed a saturation-based dimensionless time model

$$t_D = \frac{1}{L_c^2}\sqrt{\frac{K}{\Phi}}\frac{\sigma}{\mu_w S'_w + \mu_{nw} S'_{nw}}t,\ S'_w = \frac{S_w - S_{iw}}{1 - S_{rnw} - S_{iw}}$$
$$S'_{nw} = \frac{S_{nw} - S_{rnw}}{1 - S_{rnw} - S_{iw}} \tag{7}$$

3.2. Modified Ma Models. The spontaneous imbibition is conducted on the core samples from Nugget, Kentucky, Colton, and Crab Orchard under 65 °C and 18.2 MPa, and the oil recovery data are tested and illustrated in Figure 4. The experimental data of spontaneous imbibition can be fitted by the four fitting models of oil recovery in Table 3. The fitting

DOI: 10.1021/acs.energyfuels.9b01621
Energy Fuels 2019, 33, 7604−7613

Table 4. Common Formula of Dimensionless Time

research	formula	research	formula
Mattax and Kyte (1962)[41]	$t_D = \frac{1}{L_c^2}\sqrt{\frac{K}{\Phi}}\frac{\sigma}{\mu_w}t$	Cuiec et al. (1994)[42]	$t_D = \frac{1}{L_c^2}\sqrt{\frac{K}{\Phi}}\frac{\sigma}{\mu_{nw}}t$
Ma et al. (1997)[36]	$t_D = \frac{1}{L_c^2}\sqrt{\frac{K}{\Phi}}\frac{\sigma}{\sqrt{\mu_w\mu_{nw}}}t$	Ruth (2004)[43]	$t_D = \frac{1}{L_c^2}\sqrt{\frac{K}{\Phi}}\frac{\sigma}{\mu_w}a\left[1 + b\left(\frac{\mu_{nw}}{\mu_w}\right)^{1/m}\right]^{-m} t$
Li and Horne (2006)[37]	$t_D = \frac{c^2}{L_c^2}\frac{K}{\Phi}\frac{P_C\sigma}{\mu_w/K_{rw} + \mu_{nw}/K_{rnw}}t$	Fischer et al.(2008)[44]	$t_D = \frac{1}{L_c^2}\sqrt{\frac{K}{\Phi}}\frac{ab\sigma}{\mu_w + b^2\mu_{nw}}t$
Standnes (2010)[40]	$t_D = \frac{1}{L_c^2}\sqrt{\frac{K}{\Phi}}\frac{\sigma}{\mu_w^n\mu_{nw}^{1-n}}t$	Mason et al. (2010)[45]	$t_D = \frac{2}{L_c^2}\sqrt{\frac{K}{\Phi}}\frac{\sigma}{\mu_w(1 + \sqrt{\mu_{nw}/\mu_w})}t$

[a] c is tortuosity, L_c is characteristic capillary length, m, K is permeability, m^2, Φ is porosity, $\sqrt{K/\Phi}$ is characteristic value of capillary radius, m, μ_w is wetting phase viscosity, Pa·s, μ_{nw} is nonwetting phase viscosity, Pa·s, K_{rw} is the relative permeability to wetting phase, K_{rnw} is the relative permeability to nonwetting phase, and a, b, m, n are model parameters.

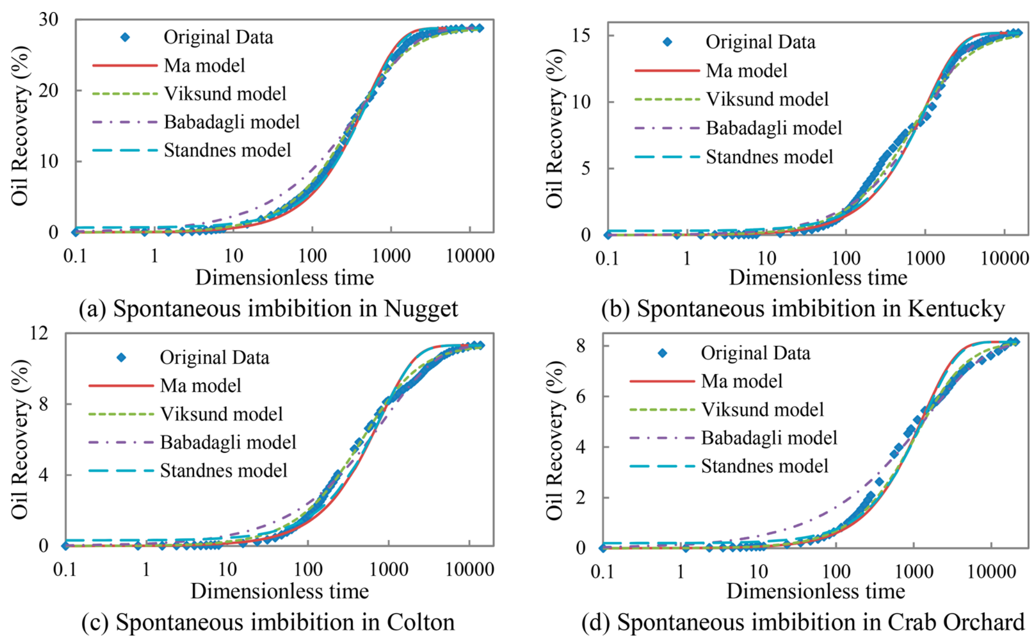

Figure 4. Oil recovery versus dimensionless time.

Table 5. Correlation Coefficients of Fitting Models on Core Samples

	Ma model		Viksund model		
core samples	λ	R^2	a	λ	R^2
Nugget	0.002246	0.9974	2.09×10^{-3}	1.377	0.9988
Kentucky	0.001203	0.9904	9.48×10^{-4}	1.593	0.9964
Colton	0.001649	0.9904	1.40×10^{-3}	1.466	0.9980
Crab Orchard	9.80×10^{-4}	0.9885	4.53×10^{-4}	2.428	0.9955

	Babadagli model			Standnes model		
core samples	ω	n	R^2	W	λ	R^2
Nugget	0.01812	0.65378	0.9949	2.6548	1.987×10^{-3}	0.9960
Kentucky	0.01845	0.79569	0.9932	2.6626	9.542×10^{-4}	0.9873
Colton	0.01166	0.65558	0.9923	2.6420	1.250×10^{-3}	0.9859
Crab Orchard	0.01670	0.56236	0.9892	2.6521	7.239×10^{-4}	0.9830

parameters and correlation coefficients are listed in Table 5, and corresponding fitting curves are drawn in Figure 4.

Because the measuring accuracy of the oil−water separator is 0.01 mL, the relative error of the measurement is about 0.0442% for core samples from Nugget (average pore volume of 22.622 mL), is about 0.0308% for Kentucky sandstone (average pore volume of 32.444 mL), is about 0.0345% for Colton sandstone (average pore volume of 28.977 mL), and is about about 0.0771% for Crab Orchard sandstone (average pore volume of 12.970 mL).

DOI: 10.1021/acs.energyfuels.9b01621
Energy Fuels 2019, 33, 7604−7613

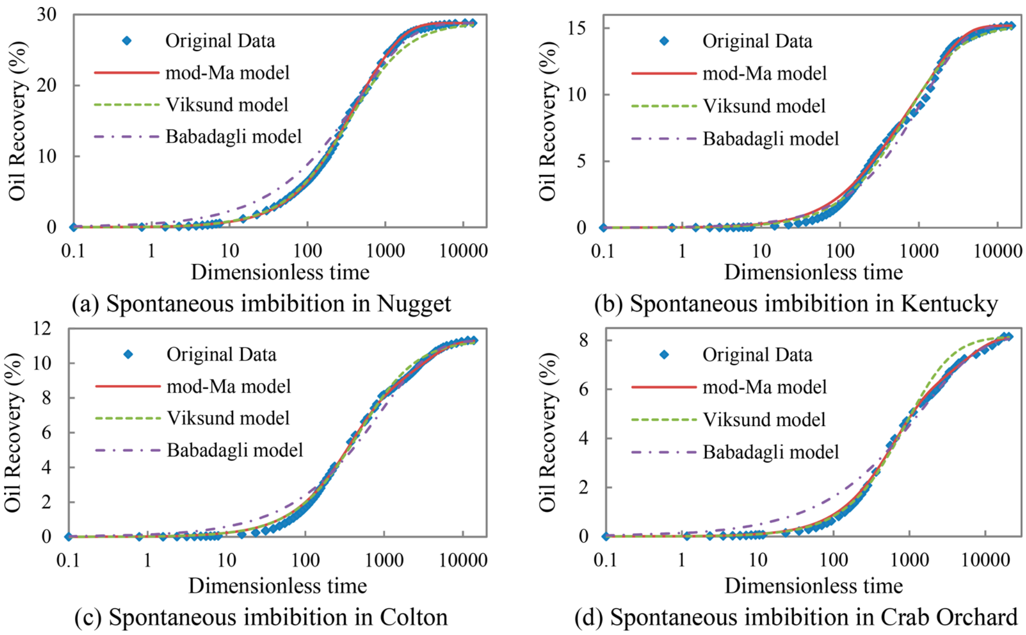

Figure 5. Oil recovery versus dimensionless time.

In Table 5, R is the correlation coefficient, defined as

$$R = \frac{\mathrm{Cov}(D_{\mathrm{Exp}}, D_{\mathrm{Fit}})}{\sqrt{\mathrm{Var}(D_{\mathrm{Exp}})\mathrm{Var}(D_{\mathrm{Fit}})}} \tag{8}$$

where D_{Exp} is experimental data, D_{Fit} is fitting data, Cov() is covariance, and Var() is variance.

According to the comparison of correlation coefficients, the Viksund model has a better fitting on the spontaneous imbibition while the Babadagli model performs better at the ending period.

Because CO_2 enhances the cocurrent imbibition strong enough, the traditional oil recovery models of spontaneous imbibition do not have a good fitting for the spontaneous imbibition of CO_2-rich brine whose imbibition rate has double peaks. For fitting the spontaneous imbibition of CO_2-rich brine, we offered a modified Ma model as

$$E_{\mathrm{R}} = E_{\mathrm{R}}^{\max}(1 - a_1 e^{-\lambda_1 t_{\mathrm{D}}} - a_2 e^{-\lambda_2 t_{\mathrm{D}}}) \tag{9}$$

where $a_1 + a_2 = 1$. When the parameter $\lambda_1 > \lambda_2$, the a_1 and λ_1 reflect the character of the countercurrent imbibition, and the a_2 and λ_2 reflect the character of the cocurrent imbibition.

The fitting curves of modified Ma model on oil recovery are illustrated in Figure 5 and Table 6.

Through comparing the correlation coefficient of modified Ma model (Table 6) to four common oil recovery models (Table 5), it is obvious that the modified Ma model can better fit the data from the spontaneous imbibition experiments of CO_2-rich brine on four typical tight rocks than traditional oil recovery models. Figure 5 illustrates that the modified Ma model is more sensible to flexibly fit the curves of oil recovery with complex imbibition rate under the influence of CO_2.

Furthermore, the parameter a_1 reflects the contribution of countercurrent imbibition to the oil recovery of spontaneous imbibition, and the a_2 reflects the contribution of cocurrent.

Table 6. Correlation Coefficients of Modified Ma Model on Core Samples

core samples	a_1	λ_1	a_2	λ_2	R^2
Nugget	0.40354	0.004684	0.59646	0.001319	0.9997
Kentucky	0.32194	0.004336	0.67806	0.000687	0.9976
Colton	0.636907	0.002958	0.363093	0.000362	0.9993
Crab Orchard	0.636627	0.001754	0.363373	0.000207	0.9989

4. RESULTS AND DISCUSSION

4.1. Influence of Porous Structure. The oil recovery and the oil production rate of spontaneous imbibition experiments on four types of core samples with different permeabilities are illustrated in Figure 6 and Figure 7.

The experimental results reflect that the spontaneous imbibition can be divided into four stages. The countercurrent imbibition is in main drive mode during the first two periods, but it weakens so rapidly after the second period that the cocurrent imbibition plays a dominate role at the later two periods.

In the initial stage, the imbibition recovery increases exponentially until the imbibition rate reaches a peak because the $scCO_2$ needs time to dissolute, diffuse, and elevate imbibition rate. For the normal oil−brine spontaneous imbibition, the imbibition rate is largest at the beginning.[15]

In the second stage that appears after the peak of imbibition rate, although the influence of CO_2 increases, the imbibition rate slows down rapidly during this period. This stage contributes to the majority part of total oil production.

At the third period, the imbibition rate reaches a plateau or recovers to another peak under the influence of CO_2. Figure 7 illustrates that the second peak of imbibition rate occurs later for the core sample with lower permeability because the mass transfer rate of CO_2 is lower in rock with lower permeability, which delays the dissolving of CO_2 in oil.

At the last period, the imbibition rate slows down and the oil recovery tends to the ultimate recovery at the end of the experiment. The tight rocks have a lengthy spontaneous imbibition under the influence of $scCO_2$. Figure 7 also illustrates that the oil production rate is very low at later period

DOI: 10.1021/acs.energyfuels.9b01621
Energy Fuels 2019, 33, 7604−7613

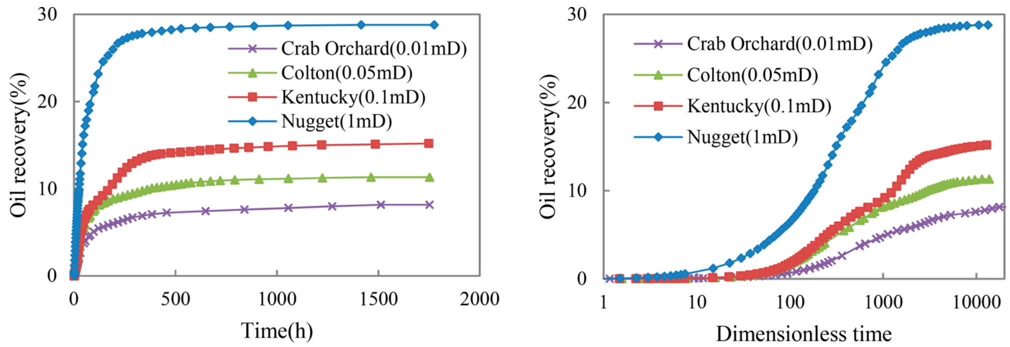

Figure 6. Oil recovery of spontaneous imbibition versus time and dimensionless time.

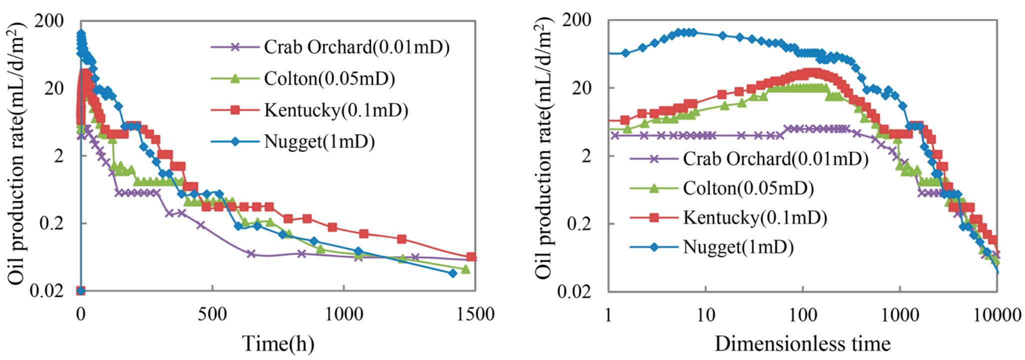

Figure 7. Oil production rate of spontaneous imbibition versus time and dimensionless time.

and has no demonstrable relationship to permeability. The imbibition rate of cocurrent imbibition is controlled by various factors, e.g., pore structure, remaining oil saturation, wettability, etc.

The viscosity of oil samples under different $scCO_2$ dissolutions is measured with capillary viscometer (S.T., Core Lab, U.S.), and the result is illustrated in Figure 8. Thus, the dissolution of CO_2 can enhance the cocurrent imbibition by reducing viscosity of oil to improve the flow capacity.

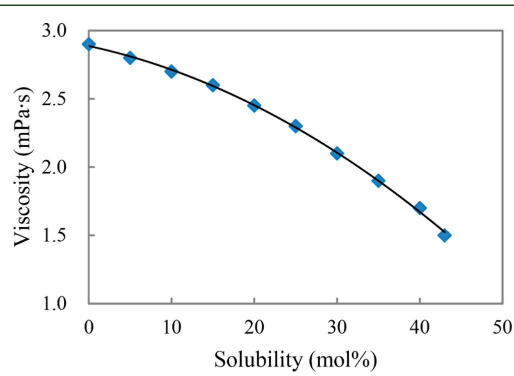

Figure 8. Viscosity of oil versus CO_2 solubility.

The results also indicate that the core sample with lower permeability has lower oil recovery and lower oil production rate. According to capillary bundle model, capillary radius is related to the group $\sqrt{K/\Phi}$.[47,46]

$$r_c \approx \sqrt{8c}\sqrt{K/\Phi} \tag{10}$$

Table 2 shows that the pore radius is smaller in the rock with lower permeability. As described in eq 4, the rock with smaller capillary size has higher capillary pressure but has much more viscous resistance and thus has lower oil production rate of countercurrent imbibition.

Table 6 shows the $a_1 < a_2$ for test on Nugget and Kentucky rocks, which indicates that the cocurrent imbibition makes more contribution than countercurrent. The $a_1 > a_2$ for test on Colton and Crab Orchard rocks indicates that the countercurrent contributes more imbibition to oil recovery. The parameter λ_2 diminishes with permeability, which implies that lower permeability postpones the second peak of imbibition rate. A main reason is that the lower permeability restrains the diffusion of CO_2 to delay cocurrent imbibition.

4.2. Influence of Pressures.

The spontaneous imbibition experiments of CO_2-rich brine are conducted on the Kentucky core samples under temperature of 65 °C and pressures of 10−22 MPa. The oil recovery and the oil production rate of spontaneous imbibition are calculated and illustrated in Figure 9 and Figure 10.

The experimental results indicate that the oil production rates under different pressure have similar trends. The spontaneous imbibition under higher pressure has higher oil production rate and higher oil recovery. Raising pressure of CO_2 can improve oil recovery of spontaneous imbibition.

The fitting curves of modified Ma model on oil recovery are illustrated in Table 7.

Table 7 shows the parameter $a_1 < a_2$ for test under the pressures in the range of 15−22 MPa, which indicates that the cocurrent imbibition makes more contribution than countercurrent. $a_1 > a_2$ under the pressure of 10 MPa, indicating the countercurrent contributes more imbibition to oil recovery. The parameter λ_1 increases with pressure, which implies that higher pressure enhanced counterimbibition to make the oil production reach the peak earlier. The parameter λ_2 is also

DOI: 10.1021/acs.energyfuels.9b01621
Energy Fuels 2019, 33, 7604−7613

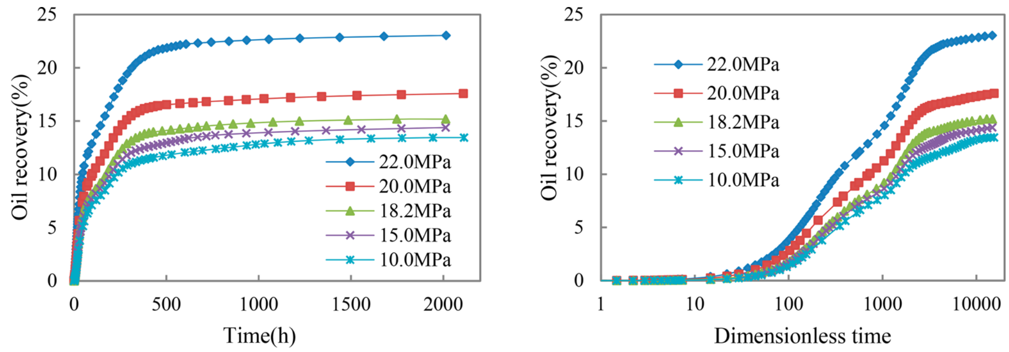

Figure 9. Oil recovery of spontaneous imbibition versus time and dimensionless time.

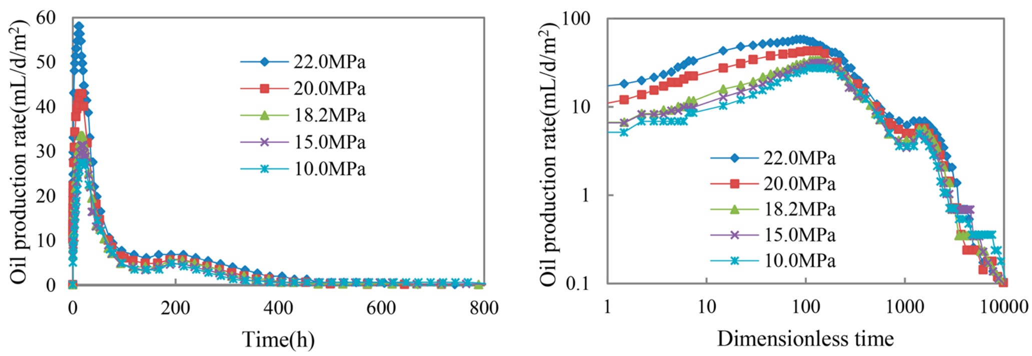

Figure 10. Oil production rate of spontaneous imbibition versus time and dimensionless time.

Table 7. Correlation Coefficients of Modified Ma Models on Core Samples

testing pressures	a_1	λ_1	a_2	λ_2	R^2
22	0.338	0.005778	0.662	0.000675	0.9986
20	0.316	0.005408	0.684	0.000744	0.9987
18.2	0.3219	0.004336	0.6781	0.000687	0.9976
15	0.4107	0.003503	0.5893	0.000548	0.9981
10	0.5219	0.002464	0.4781	0.000404	0.9984

increases with pressure, implying higher pressure also enhanced the coimbibition.

The solution of CO_2 in oil and brine can change the interfacial tensions. The equilibrium interfacial tension between CO_2-rich oil and brine is measured by pendent drop method with IFT Cell 1000 (S.T., Core Lab, U.S.) under pressures of 10−20 MPa, and the result is illustrated in Figure 11. It is reflected that elevating the pressure of $scCO_2$ can decrease the oil−water interfacial tension. According to the Young−Laplace equation (eq 1), the reducing of oil−brine interfacial tension can restrain the capillary pressure. Thus, the increase of $scCO_2$ pressure will decrease the capillary pressure without considering the change of wettability.

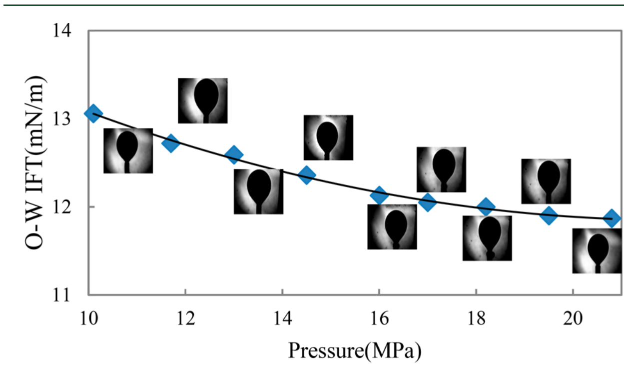

Figure 11. Interfacial tension between CO_2-rich oil and brine.

The viscosities of full-CO_2-dissolved oil under different pressures are measured with capillary viscometer (S.T., Core Lab, U.S.), and the result is illustrated in Figure 12.

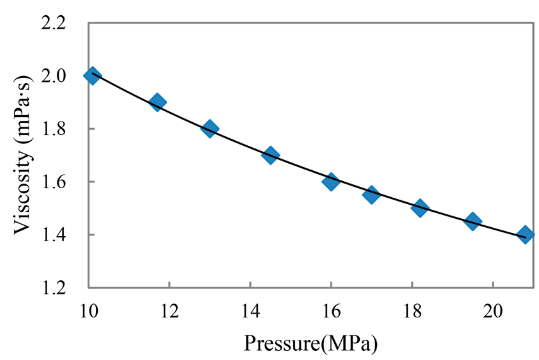

Figure 12. Viscosity of oil versus solubility.

In our previous work,[48,49] we studied the influence of water barrier on CO_2-EOR based on the microscopic experiments on ideal porous model (see Figure 13). We found that the $scCO_2$ can diffuse into oil through brine barrier. We confirmed the microscopic mechanism of CO_2-EOR on trapped oil droplets by several steps, including dissolution, swelling, extraction, and multiple contact miscibility.

Therefore, we infer that the main mechanisms of CO_2-EOR in water-flooded tight reservoir are the viscosity reducing and swelling but not the increase of capillary pressure.

DOI: 10.1021/acs.energyfuels.9b01621
Energy Fuels 2019, 33, 7604−7613

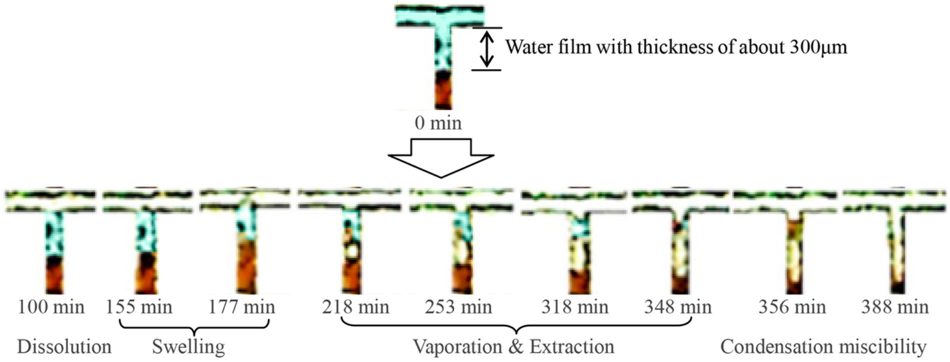

Figure 13. Process of CO_2-EOR through brine barrier (brine, blue; oil, brown; CO_2, colorless).

5. CONCLUSIONS

In this paper, we investigated the influence of CO_2 on spontaneous imbibition, which is essential to improve oil recovery in tight reservoir by migrating oil from the matrix to fracture.

- A laboratory equipment was designed to conduct spontaneous imbibition experiments at formation temperature of 65 °C and pressure of 10−22 MPa on different low-permeability core samples from Nugget, Kentucky, Colton, and Crab Orchard.
- We proposed a saturation-based dimensionless time model for scaling the spontaneous imbibition and a modified Ma model to fit the spontaneous imbibition of CO_2-rich brine whose imbibition rate has double peaks.
- The results of imbibition experiments under different permeabilities quantitatively confirm that both the oil production per unit area and the oil recovery have a positive proportional relationship with permeability. The rock with lower permeability has smaller capillary size and higher capillary pressure but has much more viscous resistance and thus has lower oil production rate of countercurrent imbibition.
- The results of imbibition experiments under different pressures quantitatively demonstrate that both the oil production and the oil recovery increase with pressure, especially when the pressure exceeds minimum miscibility pressure. A pendent drop experiment with an IFT cell illustrates that CO_2 decreases the oil−water interfacial tension with the elevating of pressure.
- The CO_2 can restrain the capillary pressure by reducing oil−brine interfacial tension but can improve the total oil recovery of spontaneous imbibition by improve flowing ability of oil by decreasing viscosity and enhancing the cocurrent imbibition through several steps, including dissolution, swelling, extraction, and multiple contact miscibility.

In summary, the results of this work suggest that application of CO_2 can lead to improved oil recovery from the fractured and water-flooded tight reservoir through spontaneous imbibition.

■ AUTHOR INFORMATION

Corresponding Author

*E-mail: luyu@btbu.edu.cn.

ORCID

Yu Lu: 0000-0002-8763-1360

Notes

The authors declare no competing financial interest.

■ ACKNOWLEDGMENTS

This work received funding from the National Natural Science Foundation of China (Grant No. 51504283), the National Key R & D Program of China (Grant No. 2016YFB0600805-1), and the Technology Development Department of SINOPEC.

■ REFERENCES

(1) Lai, F.; Li, Z.; Wei, Q.; et al. Experimental Investigation of Spontaneous Imbibition in Tight Reservoir with Nuclear Magnetic Resonance Testing. *Energy Fuels* **2016**, *30*, 8932−8940.

(2) Liu, G.; Meng, Z.; Cui, Y. A Semi-Analytical Methodology for Multiwell Productivity Index of Well-Industry-Production-Scheme in Tight Oil Reservoirs. *Energies* **2018**, *11*, 1054.

(3) Tight Oil Expected To Make Up Most of U.S. Oil Production Increase Through 2040. *U.S. Energy Information Administration, Annual Energy Outlook*, 2017. Available online: https://www.eia.gov/todayinenergy/detail.php?id=29932.

(4) Wang, H.; Lun, Z.; Lv, C.; et al. Measurement and visualization of tight rock exposed to CO_2 using NMR relaxometry and MRI. *Sci. Rep.* **2017**, *7*, 44354.

(5) Xu, J. The Largest Tight Oil Demonstration Zone in China to Boost Production. *State-owned Assets Supervision and Administration Commission of the State Council (SASAC), SOEs News*, 2018. Available online: http://www.sasac.gov.cn//n2588025/n2588124/c9506398/content (in Chinese).

(6) Xu, L.; Wang, H.; Zang, L.; et al. Research Status and Development Trend of Tight Oil in China. *Contemporary Chem. Ind.* **2017**, *46* (1), 86−88.

(7) Hao, B.; Ma, J.; Ye, B.; et al. Influencing Factors Analysis of the Horizontal Well Productivity in the Tight Reservoir of the Ordos Basin. *Well Testing* **2017**, *26* (4), 16−18.

(8) Jia, C.; Zheng, M.; Zhang, Y. Unconventional hydrocarbon resources in China and the prospect of exploration and development. *Petroleum Exploration & Development* **2012**, *39* (2), 139−146.

(9) Zuloaga-Molero, P.; Yu, W.; Xu, Y.; et al. Simulation Study of CO_2-EOR in Tight Oil Reservoirs with Complex Fracture Geometries. *Sci. Rep.* **2016**, *6*, 33445.

(10) Xuefeng, Q. U.; Fan, J.; Wang, C.; et al. Impact of Fractures on Water Flooding Seepage Features of Chang 7 Tight Cores in Longdong Area, Ordos Basin. *J. Xian Shiyou University (Nat. Sci. Ed.)* **2017**, DOI: 10.3969/j.issn.1673-064X.2017.05.009.

(11) Shen, Y.; Li, C.; Ge, H.; et al. Spontaneous imbibition in asymmetric branch-like throat structures in unconventional reservoirs. *J. Nat. Gas Sci. Eng.* **2017**, *44*, 328−337.

(12) Wang, X.; Peng, X.; Zhang, S.; et al. Characteristics of oil distributions in forced and spontaneous imbibition of tight oil reservoir. *Fuel* **2018**, *224*, 280−288.

(13) Meng, Q.; Cai, Z.; Cai, J.; et al. Oil recovery by spontaneous imbibition from partially water-covered matrix blocks with different boundary conditions. *J. Pet. Sci. Eng.* **2019**, *172*, 454−464.
(14) Khan, A. S.; Siddiqui, A. R.; Abd, A. S.; et al. Guidelines for Numerically Modeling Co- and Counter-current Spontaneous Imbibition. *Transp. Porous Media* **2018**, *124*, 743.
(15) Li, K.; Horne, R. N. Method to Evaluate the Potential of Water Injection in Naturally Fractured Reservoirs. *Transp. Porous Media* **2010**, *83* (3), 699−709.
(16) Wang, J.; Ryan, D.; Szabries, M.; Jaeger, P. A Study for Using CO_2 to Enhance Natural Gas Recovery from Tight Reservoirs. *Energy Fuels* **2019**, *33* (5), 3821−3827.
(17) Yu, W.; Lashgari, H. R.; Wu, K.; Sepehrnoori, K. CO_2 injection for enhanced oil recovery in Bakken tight oil reservoirs. *Fuel* **2015**, *159* (1), 354−363.
(18) Zhang, C.; Qiao, C.; Li, S.; Li, Z. The Effect of Oil Properties on the Supercritical CO_2 Diffusion Coefficient under Tight Reservoir Conditions. *Energies* **2018**, *11* (6), 1495.
(19) Habibi, A.; Yassin, M. R.; Dehghanpour, H.; et al. Experimental investigation of CO_2-oil interactions in tight rocks: A Montney case study. *Fuel* **2017**, *203*, 853−867.
(20) Mohammad, R. S.; Zhang, S.; Zhao, X.; Lu, S. An Experimental Study of Cyclic CO_2-Injection Process in Unconventional Tight Oil Reservoirs. *Oil & Gas Research* **2018**, *04* (01) DOI: 10.4172/2472-0518.1000150.
(21) Wang, R.; Lv, C.; Yue, X.; et al. Experimental study on the effects of carbonate water on rock wettability and imbibition recovery. *J. Xi'an Shiyou University (Nat. Sci. Ed.)* **2010**, *25*, 48−50.
(22) Yang, D.; Song, C.; Zhang, J.; et al. Performance evaluation of injectivity for water-alternating-CO_2 processes in tight oil formations. *Fuel* **2015**, *139*, 292−300.
(23) Ren, B.; Zhang, L.; Huang, H.; Ren, S.; Chen, G.; Zhang, H. Performance evaluation and mechanisms study of near-miscible CO_2 flooding in a tight oil reservoir of Jilin Oilfield China. *J. Nat. Gas Sci. Eng.* **2015**, *27*, 1796−1805.
(24) Pu, W.; Wei, B.; Jin, F.; Li, Y.; Jia, H.; Liu, P.; Tang, Z. Experimental investigation of CO_2 huff-n-puff process for enhancing oil recovery in tight reservoirs. *Chemical Engineering Research & Design* **2016**, *111*, 269−276.
(25) Gong, Y.; Gu, Y. Experimental Study of Water and CO_2 Flooding in the Tight Main Pay Zone and Vuggy Residual Oil Zone of a Carbonate Reservoir. *Energy Fuels* **2015**, *29* (10), 6213.
(26) Ma, J.; Wang, X.; Gao, R.; et al. Enhanced light oil recovery from tight formations through CO_2 huff 'n' puff processes. *Fuel* **2015**, *154*, 35−44.
(27) Cui, M.; Wang, R.; Lv, C.; Tang, Y. Research on microscopic oil displacement mechanism of CO2 EOR inextra-high water cut reservoirs. *J. Pet. Sci. Eng.* **2017**, *154*, 315−321.
(28) Tian, X.; Cheng, L.; Cao, R.; et al. Potential evaluation of CO_2 storage and enhanced oil recovery of tight oil reservoir in the Ordos Basin, China. *J. Environ. Biol.* **2015**, *36* (4), 789−797.
(29) Riazi, M. *Pore scale mechanisms of carbonated water injection in oil reservoirs.* Ph.D. Thesis, Heriot-Watt University, 2011.
(30) Zhang, W.; Xie, L.; Yang, W.; et al. Micro fractures and pores in lacustrine shales of the Upper Triassic Yanchang Chang7Member, Ordos Basin, China. *J. Pet. Sci. Eng.* **2017**, *156*, 194−201.
(31) Ma, F.; Li, Y.; Ge, Y.; et al. Evaluation on Effective Source Rock of Tight Oil in Yanchang Formation, Ordos Basin. *Special Oil & Gas Reservoirs* **2017**.
(32) Wang, F., Wei, Y., Chen, C. Forming mechanisms of reservoir "sweet spots"in tight sandstones of Chang8 Formation, Honghe oil field, Ordos Basin. *Petroleum Geology & Experiment* **2017**, *39* (4).
(33) Jia, J.; Yin, W.; Qiu, N.; et al. Quantitative characterization of migration system of Yanchang Formation in Honghe oil field, Ordos Basin. *Oil & Gas Geology* **2017**, *38* (5), 878−886.
(34) Mingpei, W.; Dongling, X.; Yue, W. U.; et al. Diagenesis features of Chang 8 tight sandstone reservoir in Honghe oil field, Ordos Basin. *Petroleum Geology & Experiment*, **2018**, *40*(6).
(35) Jia, J.; Yin, W.; Qiu, N. Migration and accumulation of crude oil in Upper Triassic tight sand reservoirs on the southwest margin of Ordos Basin, Central China: A case study of the Honghe Oilfield. *Geol. J.* **2018**, *53* (5), 2280.
(36) Wang, Q.; Qin, Y.; Jia, W.; Wang, Y.; Zhang, W.; Peng, P.a. Density and viscosity of tight oil from Yanchang Formation, Ordos Basin, China and the geochemical controls. *Pet. Sci. Technol.* **2018**, *36*, 1298.
(37) Wang, Q. Geochemical characteristics and genesis of tight and shale oil from the 7th Member of Yanchang Formation in Ordos Basin. *Univ. Chin. Acad. Sci.* **2018**.
(38) Wei, M.; Tang, H.; Lv, D.; et al. The research of experimental about different flooding velocity on imbibition. *Petrochem. Ind. Appl.* **2015**, *34* (3), 20−22.
(39) Shouxiang, M.; Morrow, N. R.; Zhang, X. Generalized scaling of spontaneous imbibition data for strongly water-wet systems. *J. Pet. Sci. Eng.* **1997**, *18* (3−4), 165−178.
(40) Li, K.; Horne, R. N. Generalized Scaling Approach for Spontaneous Imbibition: An Analytical Model. *SPE Reservoir Evaluation & Engineering* **2006**, *9* (03), 251−258.
(41) Viksund, B. G.; Morrow, N. R.; Ma, S. Initial water saturation and oil recovery from chalk and sandstone by spontaneous imbibition. International Symposium of the Society of Core Analysts, 1998; SCA1998-14, Vol. 1, pp 1−9.
(42) Babadagli, T.; Hatiboglu, C. U.; Hamida, T. Evaluation of Matrix-Fracture Transfer Functions for Counter-Current Capillary Imbibition. *Transp. Porous Media* **2009**, *80* (1), 17−56.
(43) Standnes, D. C. Scaling spontaneous imbibition of water data accounting for fluid viscosities. *J. Pet. Sci. Eng.* **2010**, *73* (3), 214−219.
(44) Mattax, C. C.; Kyte, J. R. Imbibition Oil Recovery from Fractured, Water-Drive Reservoir. *SPEJ, Soc. Pet. Eng. J.* **1962**, *2* (02), 177−184.
(45) Cuiec, L. E.; Bourbiaux, B.; Kalaydjian, F. Oil Recovery by Imbibition in Low-Permeability Chalk. *SPE Form. Eval.* **1994**, *9* (03), 200−208.
(46) Ruth, D. W.; Mason, G.; Morrow, N. The effect of fluid viscosities on counter-current Spontaneous Imbibition. International Symposium of the Society of Core Analysts, Abu Dhabi, 2004; SCA2004-11, pp 1−13.
(47) Fischer, H.; Wo, S.; Morrow, N. R. Modeling the Effect of Viscosity Ratio on Spontaneous Imbibition. *SPE Reservoir Evaluation & Engineering* **2008**, *11* (03), 577−589.
(48) Mason, G.; Fischer, H.; Morrow, N. R.; et al. Correlation for the effect of fluid viscosities on counter-current spontaneous imbibition. *J. Pet. Sci. Eng.* **2010**, *72* (1−2), 195−205.
(49) Wu, K.; Liu, L.; Xu, Z. Lower limits of pore throat radius, porosity and permeability for tight oil accumulations in the Chang7Member, Ordos Basin. *Petroleum Geology & Experiment* **2016**, *38* (1), 63−69.

DOI: 10.1021/acs.energyfuels.9b01621
Energy Fuels 2019, 33, 7604−7613